

An optimization framework for curvilinearly stiffened composite pressure vessels and pipes

Karanpreet Singh*, Wei Zhao^a and Rakesh K. Kapania^b

*Kevin T. Crofton Department of Aerospace and Ocean Engineering,
Virginia Polytechnic Institute and State University, Blacksburg, Virginia 24060, U.S.A.*

(Received November 10, 2019, Revised April 7, 2020, Accepted July 28, 2020)

Abstract. With improvement in innovative manufacturing technologies, it became possible to fabricate any complex shaped structural design for practical applications. This allows for the fabrication of curvilinearly stiffened pressure vessels and pipes. Compared to straight stiffeners, curvilinear stiffeners have shown to have better structural performance and weight savings under certain loading conditions. In this paper, an optimization framework for designing curvilinearly stiffened composite pressure vessels and pipes is presented. NURBS are utilized to define curvilinear stiffeners over the surface of the pipe. An integrated tool using Python, Rhinoceros 3D, MSC.PATRAN and MSC.NASTRAN is implemented for performing the optimization. Rhinoceros 3D is used for creating the geometry, which later is exported to MSC.PATRAN for finite element model generation. Finally, MSC.NASTRAN is used for structural analysis. A Bi-Level Programming (BLP) optimization technique, consisting of Particle Swarm Optimization (PSO) and Gradient-Based Optimization (GBO), is used to find optimal locations of stiffeners, geometric dimensions for stiffener cross-sections and layer thickness for the composite skin. A cylindrical pipe stiffened by orthogonal and curvilinear stiffeners under torsional and bending load cases is studied. It is seen that curvilinear stiffeners can lead to a potential 10.8% weight saving in the structure as compared to the case of using straight stiffeners.

Keywords: pressure vessels; curvilinear stiffeners; optimization framework; finite element analysis

1. Introduction

Pressure vessels and pipes are integral parts of many industries like oil refineries, chemical and nuclear industries etc. The important loads to design these vessels and pipes are internal and external pressure (vacuum inside) and boundary loads such as bending moment, axial compression and torsion. Design temperature is also an important variable for pressure vessels and piping (Parnas and Katircı (2002)). Modern developments in manufacturing technologies have made it possible to manufacture high complexity shapes and designs. High performance computing and commercial software such as MSC.NASTRAN, MSC.PATRAN have the capability to both

*Corresponding author, Ph.D., E-mail: kasingh@vt.edu

^aPost-Doctorate Fellow, E-mail: weizhao@vt.edu

^bMitchell Professor, Email: rkapania@vt.edu

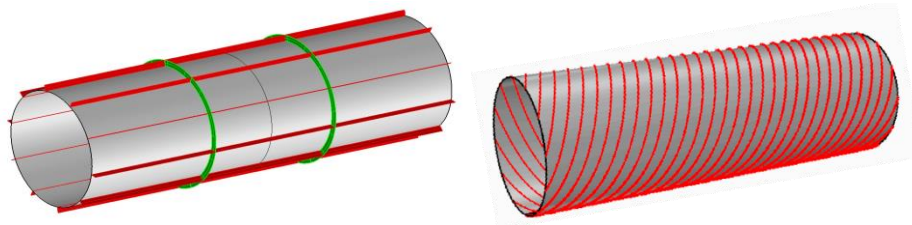


Fig. 1 (Left) Orthogonal stiffeners. (Right) Curvilinear Stiffeners

analyze and optimize a large class of such designs. Arbitrary-shaped geometries of these components have become possible using commercially available modeling software, such as Rhinoceros 3D, using Non-Uniform Rational B-Splines (NURBS). Advancements in manufacturing, designing and analysis capabilities have made it possible to design curvilinearly stiffened plates and shells for practical applications.

In past decades, extensive research was conducted on the design and analysis of pressure vessels and pipes. Dorey *et al.* (1999) experimentally investigated the bending and axial strain capacity of metallic pipelines under combined axial compression, bending and internal pressure. Their experimental tests involved pressurizing a section of a pipe and then putting a compressive load on it, until it failed. The load is applied either along the pipe axis or eccentrically in order to apply additional bending. Limam *et al.* (2010) investigated the problem of inelastic bending and the collapse of elasto-plastic tubes in the presence of internal pressure using experiments and computational analysis. They presented results where small wrinkles appeared on the compressed side of the tube whose amplitude grew stably as bending progressed, eventually causing failure. Parnas and Katirci (2002) developed an analytical procedure to design and predict the behavior of fiber-reinforced composite pressure vessels under various loading conditions. They considered internal pressure, axial and body forces due to rotation in addition to temperature and moisture variation throughout the body. Paquette and Kyriakides (2006) studied plastic buckling and collapse of long metallic cylinders under combined internal pressure and axial compression through experiments and analyses. They have shown that under continued compression, the wrinkles grew stably on the surface, eventually leading to limit load instability.

In past decade, a significant research has been conducted for using composites in the design of pressure vessels and pipes. Krikanov (2000) presented a new method to design laminated composite pressure vessels under strain and strength constraints. Their method is based on finding optimal layer thickness for given fiber orientations. Colombo and Vergani (2018) developed analytical tool for optimal design of composite pipes. They stated that composite materials could avoid issues of corrosion and maintenance. Liu, Wei and Gao (2019) presented a novel structure of woven composite pressure pipes and its multi-scale analysis. They showed that their concept can improve the bearing capacity of the composite pressure pipes.

In literature, different approaches are used for optimizing composite pressure vessels and pipes. Alcantar *et al.* (2017) conducted optimization of composite pressure vessels using genetic algorithms (GA) and simulated annealing (SA). Their objective function is based on Tsai-Wu failure criterion. They subjected the laminate to in-plane loads. They indicated that GA and SA reach similar optimal solutions irrespective of the number of layers. Chen *et al.* (2018) presented a novel reliability-based two level optimization method for composite laminated structures. Their approach consists of layer thickness and stacking sequence optimizations, where uncertain

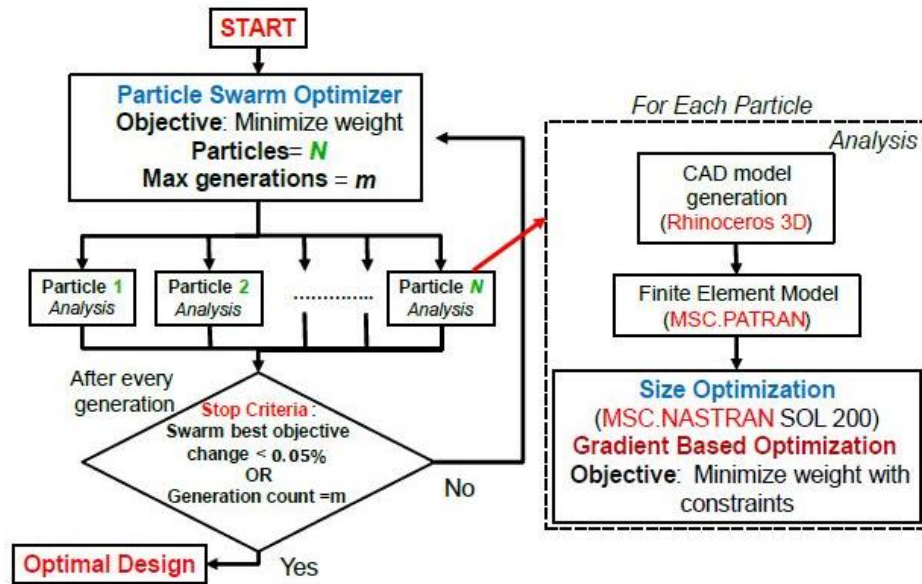


Fig. 2 Flowchart of global optimization

parameters of composites are used for reliability evaluation.

The conventional stiffeners for pressure vessels are straight stiffeners in the longitudinal direction and rings in the circumferential direction. In order to enhance the design space, one might consider curved stiffening members as shown in Fig. 1. During the last decade, significant research has been conducted on the use of curvilinear stiffeners for designing stiffened plates and shells. Kapania *et al.* (2005) have shown that curvilinear stiffened panels lead to lighter weight designs than panels with straight stiffeners under certain design loads. Zhao and Kapania (2016) studied the buckling response of curvilinearly stiffened composite plates subjected to various in-plane loads. Their research shows that the buckling response can be improved using curvilinear stiffeners in addition to tailoring the laminate configurations. Kidane *et al.* (2003) conducted buckling load analysis by developing an analytical model for the determination of equivalent stiffness parameters of a grid-stiffened composite cylindrical shell.

2. Methodology

The current work is focused on utilizing and evaluating the different capabilities of various commercially available software to solve the problem at hand. This enables the analysis of curvilinearly stiffened pipes with the objective of minimizing the structural weight by optimizing stiffener placement and their cross-section.

2.1 Procedure

In this paper, the geometry has been represented by NURBS (Non-Uniform Rational B-Splines). A commercially available geometric modeling software, Rhinoceros 3D, is used to generate a

NURBS-based CAD model for a stiffened pipe. The geometry is then exported in IGES format to MSC.PATRAN. MSC.PATRAN's built-in native language, Patran Command Language (PCL), is used to generate session files. The session file can be used to perform finite element analysis multiple times for geometries with different dimensional parameters. Finally, the obtained mesh along with the applied loads are passed onto MSC.NASTRAN for linear static and buckling analysis. A Python script is written to control the complete optimization process. The flowchart of the global optimization is shown in Fig. 2. The optimization is conducted based on BLP optimization technique. At upper level, PSO is used to minimize the weight of the structure without any constraints. At lower level, GBO is used to minimize the weight under buckling, stiffener's stress and composite skin failure index constraints. The optimization starts with an initial set of values, $Xsize$, for the cross-section of the stiffeners and the pipe's surface thickness. The stiffener placement shape design variables are denoted by $Xshape$ in this paper. The range of $Xshape$ along with the initial user-defined values of $Xsize$ are provided to the PSO. The details of the PSO are mentioned in the Section 2.2. For each particle of the PSO, size optimization using GBO has been implemented to optimize the stiffener thickness and shell thickness ($Xsize$) for a given fixed stiffener shape design ($Xshape$). Therefore, for each particle of the PSO, an optimal size design is obtained. Zhao and Kapania (2019) utilized a similar technique to optimize the internal structural layout of a composite aircraft wing. Compared to a two-step optimization approach (Singh, Zhao and Kapania (2017)) where PSO was used for shape optimization and then GBO was used separately for size optimization, the presented BLP based single step optimization approach converges faster (Zhao and Kapania (2019)).

2.2 Global optimization

The global optimization framework is shown in Fig. 1. In PSO, the objective of the optimization is to minimize the weight, $f(x)$, without any constraints as shown in Eq. (1). The a and b denote bounds on x and x_h is a h^{th} design variable

$$\text{Objective function: Minimize}(f(x)), a_h \leq x_h \leq b_h \quad h = 1, 2, \dots, n \quad (1)$$

In this optimization, a set of random particles uniformly distributed, known as designs in the present problem, are defined over the full domain of design variables. The design variables are shape design variables, $Xshape$, in our case. The objective function is evaluated for every particle. The required number of particles, N , and the maximum possible generations, m , can be set by the user according to the number of design variables. The design variables of the particle are updated based on the best particle in the swarm with the best fitness function. After each generation, updated values of the design variables are evaluated for finding the required value of the objective function.

Fig. 2 shows a complete PSO iteration. For the first iteration, PSO generates its own N particles depending upon the user input values. For each particle, Rhinoceros 3D is called to generate the required CAD model through *Rhino.Python*, which is then exported to MSC.PATRAN for generating the mesh along with the boundary conditions and applied loads. MSC.NASTRAN then conducts the structural analysis and size optimization. The objective of the size optimization is to minimize the weight with user-defined constraints, such as buckling, stiffener's stress and composite skin failure index. The GBO (MSC.NASTRAN SOL 200) would optimize composite skin laminate thickness and stiffener cross-section while satisfying the constraints. There can be some cases where the GBO could not converge to an optimal feasible design or if MSC.PATRAN

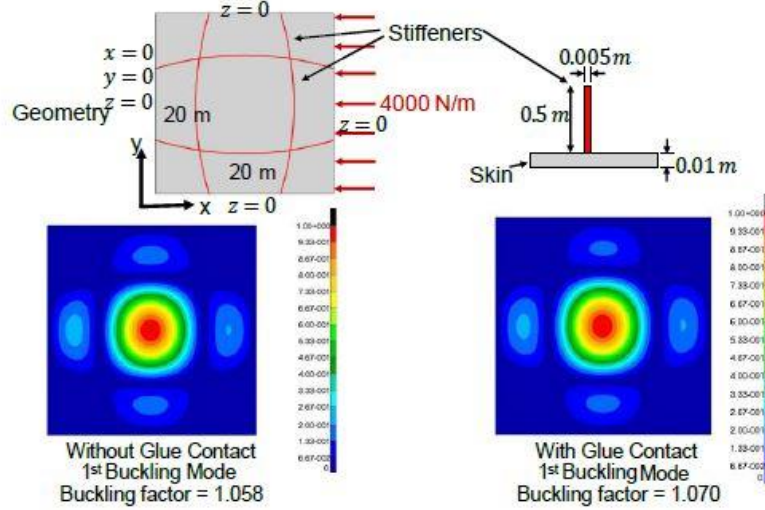


Fig. 3 Verification study of glue contact

could not successfully generate a mesh for a model. In these specific cases, a penalty is given to the objective function in PSO by providing a very large value to that particle in the swarm. Otherwise, no penalty is added to the objective function.

2.2 Verification study for glue contact capability

In the present work, a built-in capability of MSC.NASTRAN known as *Glue Contact* has been used to define contact between the surface of the skin and the stiffeners to satisfy the equilibrium and compatibility conditions. This capability has the advantage of placing stiffeners arbitrarily on the skin of the pipe. This eliminates the need for coincident nodes at stiffener-shell interfaces. The technology can be applied as linear contact where two bodies remain in contact in any condition. It is also possible to provide a very large value ($1e20$) of frictional shear stress, for the stiffener-shell interfaces when using *Glue Contact*, in MSC.NASTRAN in order to avoid any failure of contact between the bodies. Initially, in order to verify this capability, a simple verification study was conducted with an arbitrary model. A plate with curvilinear stiffeners on its surface has been considered. Figure 3 shows the results from the model using *Glue Contact*, where the stiffeners and the skin have dissimilar meshes, meaning the nodes of stiffeners and skin do not coincide at the interface. The results are compared to an equivalence model, where the nodes of the stiffener and shell elements coincide at the shell-stiffener interfaces. It can be seen that results between the two methods vary very slightly, just a slightly more than 1%.

3. Parameterization of stiffener placement

3.1 Parameterization process

In this paper, a stiffener's initial placement is defined in a 2D base reference plane, with corners

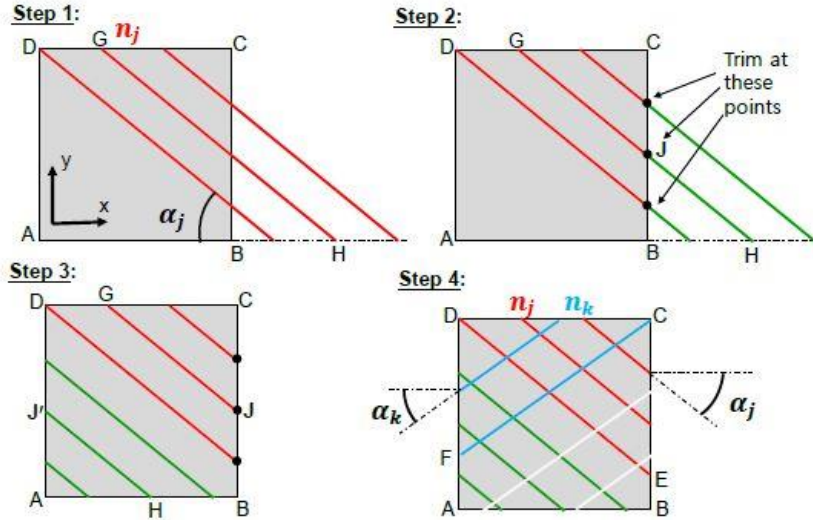


Fig. 4 Parameterization of the stiffeners placement on 2D base reference plane

A, B, C and D, as shown in Fig. 4. To parameterize a grid of curvilinear stiffeners, four parameters have been defined; n_j , n_k , α_j and α_k . The parameters, n_j and n_k represent the number of curves or stiffeners, and α_j , α_k represent the tangents of these curves respectively. In Step 1: a curve is defined starting from D at an angle α_j as specified by the user. Later, the $n_j - 1$ remaining curves are defined by offsetting the first initially defined curve by a distance, (DC/n_j) , in the positive x-direction along the edge DC. The parameter α_j is only allowed to vary from 0° to 90° . In Step 2, all curves which are going out of the reference surface are identified and trimmed at the intersection with the edge BC. For example, in Fig. 4, the curve GH is intersecting BC at J. In Step 3, all the trimmed curves outside the reference surface are identified and translated in the negative x-direction with a distance equal to DC. After translation of the trimmed curves, shown in green, a new point J' is formed. If any of the new curves still intersect BC, the same procedure (Steps 1-3) is repeated until there are no curves outside of the reference surface. In Step 4, a complete grid is defined by repeating Steps 1-3, but in the opposite direction. A curve is defined starting from C at an angle α_k , as specified by the user. Later, the $n_k - 1$ curves are defined by offsetting the first curve with the distance, DC/n_k , in the negative x-direction. The parameter, α_k is only allowed to vary from 0° to 90° . All curves that are going out of the reference surface are identified and trimmed at the intersection with the edge AD. Later, all the trimmed curves (shown in white color in Fig. 4) are translated towards positive x-direction with the distance equal to edge DC. The parameterization is implemented by writing a Python script that is run in Rhinoceros 3D using its feature of *Rhino.Python*.

3.2 Transformation of stiffeners from reference surface to physical surface

After the definition of the stiffeners in 2D base reference surface, the stiffeners are transformed onto a physical surface as shown in Fig. 5. The 2D base rectangular surface is folded to make a cylindrical surface. In the figure, the rectangular surface ABCD has been folded and the edges AB and CD have been joined. With the presented parameterization, the stiffeners automatically match

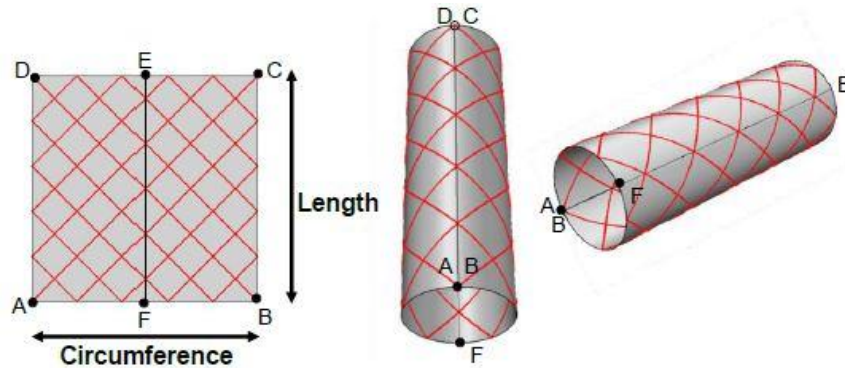


Fig. 5 Transformation of stiffeners from reference surface to physical surface

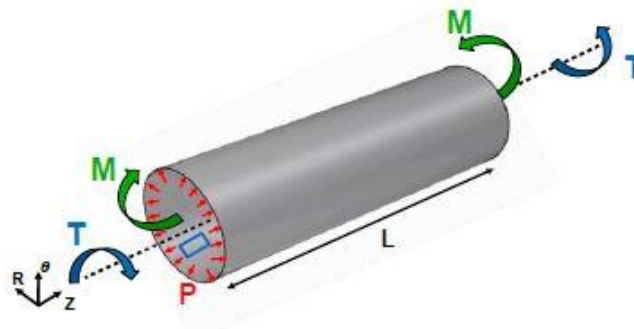


Fig. 6 Problem description

at the joining edge. It can be seen that the edge AB became the circumference of the cylindrical surface and the edge BC became the length of the cylinder. The transformation has the advantage of transforming stiffeners to any complexly-shaped surface. The transformation has been implemented in Rhinoceros 3D using the command *FlowAlongSrf*. This command can map any curve from a source surface to a target surface.

4. Problem description

In this paper, a stiffened cylindrical pipe or pressure vessel is studied. Figure 6 shows the boundary applied loading under simply supported boundary conditions. A cylindrical coordinate system is used for defining the geometry. Two load cases have been considered as 1) an in-plane bending moment (M) along with an internal pressure (P) 2) a torque (T) along with internal pressure (P) have been considered as shown in the figure. Limam *et al.* (2010) stated that in earthquake prone areas, where landslides could cause ground movements, can also place the pipes under bending and compression along with internal pressure. Also, an aircraft fuselage is subjected to internal pressure, bending and torsional loads. With this motivation, we considered internal pressure and torque or moments while developing the optimization framework. A three-layered composite laminate has been considered to define the material of the skin. The structure is

designed under these two load cases with the objective of minimizing the weight.

The objective of the presented research is to develop a general computational framework where user can design curvilinearly stiffened pressure vessels and pipes. In the framework, the user can change different properties related to structural design. For example, pipe's dimensions, material properties, element length in finite element model, etc. The required element length in the finite element model would be different for different designs. The framework is validated in a way that it successfully creates CAD geometry, mesh generation for finite element model and required NASTRAN analysis. We are using commercialized software in CAD geometry generation, mesh generation and structure analysis. The Particle Swarm Optimizer (PSO) has been verified by using some benchmark optimization problems. The user would have to select appropriate element length for structures with different dimensions and load cases.

5. Applications and results

In this section, the methodology, explained in Section 2, has been applied to study different stiffener configurations. The optimization is performed using parallel processing (Singh *et al.* (2019)). The fact that the function evaluations in PSO are independent to each other allows for the use of parallel computation at each iteration and results in a significantly less computer run-time. The machines used in these studies have 2.2 GHz AMD Opteron Processors, at least 132 GB of RAM, and 48 CPUs.

In a first load case, a bending moment (M in Fig. 6) of 250 kN-m and an internal pressure (P in Fig. 6) of 100 kPa is applied on the structure. In a second load case, a torque (T in Fig. 6) of 250 kN-m and an internal pressure (P) of 100 kPa is applied on the structure. There could be many load cases beyond the scope of this paper. The radius and the length of the pipe are 0.5 m and 3.14 m respectively. The length of the pipe has been set equal to the circumference for this problem. Two different stiffener configurations have been studied as follows: 1) Orthogonal stiffeners (conventional stiffeners); 2) Curvilinear stiffeners. The presented framework is designed such that the user could change the type of the applied loads at the ends of the pipe. The current studies demonstrate the use of the presented framework under two load cases. The framework is capable of designing pressure vessel and pipes under internal pressure, axial loads, shear loads and moment loads.

The skin of the cylinder is modeled with the composite laminate with woven fabric. The properties of the composite laminate material are mentioned in Table 1. An isotropic material, aluminum alloy Al 2139, has been considered for the stiffeners. The material properties for the isotropic material are shown in Table 2. The skin mesh is kept same in all the stiffener configurations studied in this paper. MSC.NASTRAN "CTRIA3" triangular shell elements are used for modeling both the skin and the stiffeners. During mesh generation of skin of the cylinder in MSC.PATRAN, the average element edge length is set to 0.02 m for a converged result. For stiffeners, three elements through the height of the stiffener are used. The number of elements of different models could vary from 50,000 to 250,000 depending upon the number of stiffeners in the structure. The time taken by the GBO for size optimization of the structure depend upon the mesh size, the CPU configurations and how close the initial guesses for the design variables are from the local optima for any particular model. The time taken by GBO could vary from 10 min to 1.5 hours for optimizing the structure. In the presented studies, optimization wall-clock time varied from 20-30 hours while making use of parallel processing. Thus, this is a computationally

Table 1 Mechanical properties for composite laminate (carbon fiber) used for modeling skin

Property	Value
Elastic modulus E_{11} (GPa)	70
Elastic modulus E_{22} (GPa)	70
Shear modulus G_{12} (GPa)	5
Major Poisson's ratio ν_{12}	0.1
Ultimate tensile strength in 1-dir (MPa)	600
Ultimate comp strength in 1-dir (MPa)	570
Ultimate tensile strength in 2-dir (MPa)	600
Ultimate comp strength in 2-dir (MPa)	570
Ultimate in-plane shear strength (MPa)	90

Table 2 Isotropic material used for modeling skin

Material (Aluminum Alloy)	Al 2139
Young's Modulus (E) (GPa)	73.085
Poisson ratio	0.33
Allowable stress (MPa)	427.47

expensive problem.

5.1 Constraints

The buckling factor, λ , is defined as the ratio of the buckling load of the structure to the applied load. Due to in-plane bending, there can be wrinkling (Limam *et al.* 2010) on the compressed side of the pipe. Also, the pipe could buckle under applied torque. Thus, a buckling constraint has been considered during optimization. In order to consider the failure of the composite laminate, the *Tsai–Wu* failure criterion has been used. According to the criterion, if the Failure Index (F.I.) < 1, then the composite laminate is safe. Also, a stress factor, defined as a ratio of the maximum von Mises stress and the yield stress (σ_y), is found for the stiffeners. Therefore, three constraints have been defined as

- Buckling Factor (λ) > 1
- Failure Index (F.I.) < 1
- Stress Factor (Stiffeners) < 1

The failure criterion constraint has been applied to each layer of the composite laminate. All the constraints are defined in MSC.PATRAN and are provided to MSC.NASTRAN for size optimization.

5.2 Orthogonal stiffeners

In this section, the results of application of the methodology using orthogonal stiffeners under torsional and bending load cases are presented.

Design Variables:

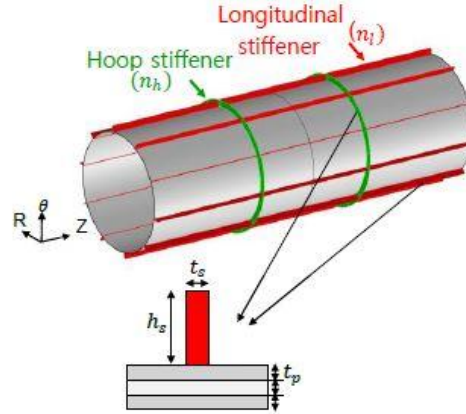


Fig. 7 Orthogonal stiffeners

Table 3 Range of X_{shape} for orthogonal stiffeners

	Lower Bound	Upper Bound
n_h	1	20
n_l	1	20
h_s (m)	0.005	0.05

Table 4 Range of X_{size} design variables

	Lower Bound	Upper Bound
t_s (m)	0.001	0.01
t_p (m)	0.0001	0.01

Fig. 7 shows the different design variables that have been used to define the orthogonal stiffeners.

n_h : Number of hoop stiffeners

n_l : Number of longitudinal stiffeners

t_s : Thickness of the stiffener

h_s : Height of the stiffener

t_p : Thickness of the each layer of composite laminate

The optimization starts with some user-input values of the size design variables, X_{size} , which includes t_s and t_p . The shape design variables, X_{shape} , include n_h , n_l and h_s . The PSO is provided with the domain of X_{shape} as shown in the Table 3. The GBO is provided with the range of X_{size} design variables as shown in Table 4.

The optimal configuration with straight stiffeners is shown in Fig. 8 for the torsional load case. The buckling factor of optimal configuration is 1.000 and the maximum failure index is 0.913. The stress factor is 0.995. This shows that buckling and stress factor constraints are both active in the optimal design. The mass of the optimal structure is 36.48 kg. The optimal configuration shows that adding longitudinal stiffeners could be more helpful in saving weight as compared to addition of hoop stiffeners. The optimal configuration with straight stiffeners for the bending load case is

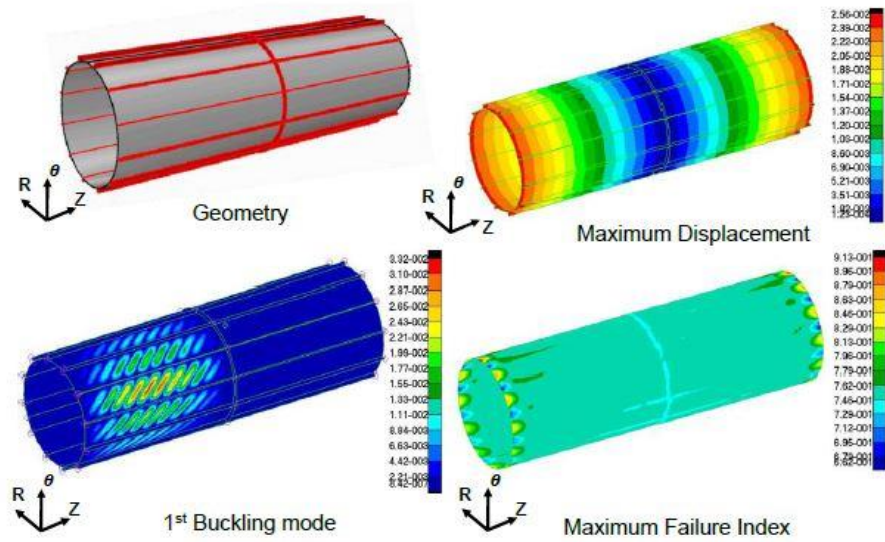


Fig. 8 Optimal configuration using orthogonal stiffeners under the torsional load case. ($n_h=1, n_l=12$, buckling factor=1.000, maximum failure index=0.913, stress factor (stiffeners)=0.995, mass=36.48 kg) the optimal cross-section dimensions are given in Table 5

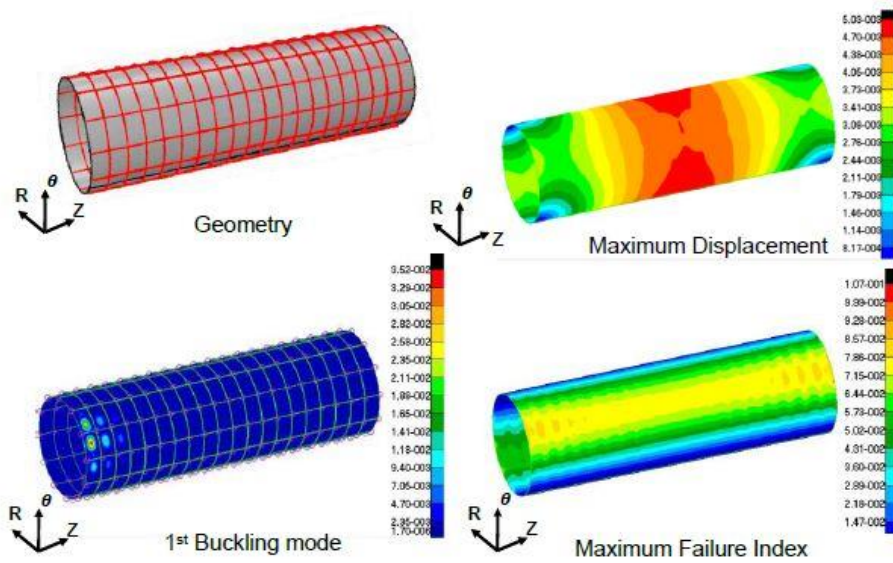


Fig. 9 Optimal configuration using orthogonal stiffeners under the bending load case. ($n_h=19, n_l=12$, buckling factor=0.999, maximum failure index=0.107, stress factor (stiffeners)=0.813, mass = 36.10 kg) the optimal cross-section dimensions are given in Table 5

shown in Fig. 9. In this configuration, only the buckling constraint is active with the buckling factor of 0.999. The maximum failure index and stress factor are 0.107 and 0.813. The optimal mass of the structure in the bending load case is 36.10 kg. It can be seen that local buckling occurs

Table 5 Optimal final values of design variables for the orthogonal stiffeners case

	Torsional Load Case	Bending Load Case
n_h	1	19
n_l	12	12
h_s (m)	3.914E-02	1.067E-02
t_s (m)	1.000E-03	1.000E-03
t_p (m)	6.788E-04	7.025E-04
Mass (kg)	36.48	36.10

Table 6 Range of $Xshape$ for curvilinear stiffeners

	Lower Bound	Upper Bound
n_j	1	17
n_k	1	17
α_j (degrees)	22.5	90
α_k (degrees)	22.5	90
h_s (m)	0.005	0.05

in the skin. Also, in comparison to the torsional load case, in the bending load case adding both hoop and longitudinal stiffeners could help in reducing the weight. The optimal values of the design variables are tabulated in Table 5

5.3 Curvilinear stiffeners

In this section, the results from application of the methodology using curvilinear stiffeners are presented.

Design Variables:

Fig. 4 shows the different design variables that have been used to define the curvilinear stiffeners. In Fig. 4, $AB=BC=CD=DA$. The size design variables in this section are same like that of case of orthogonal stiffeners.

n_j : Number of stiffeners in the direction from left to right

n_k : Number of stiffeners in the direction from right to left

α_j : Orientation angle of n_j stiffeners

α_k : Orientation angle of n_k stiffeners

As stated above, the optimization starts with user-input values of the size design variables, $Xsize$. $Xsize$ includes h_s and t_p . The shape design variables, $Xshape$, includes n_j , n_k , α_j , α_k and h_s . The PSO is provided with the domain of $Xshape$ as shown in the Table 6. The GBO is provided with the range of $Xsize$ design variables as shown in Table 4. The parameters α_j and α_k , shown in Fig. 4, can vary from 22.5° to 90° .

Fig. 10 shows the optimal configuration using curvilinear stiffeners under torsional load case. The buckling constraint is active with the buckling factor of 1.004. The maximum failure index and stress factor are 0.869 and 0.822. The optimal weight of this configuration is 38.26 kg. This optimal weight is very close to the optimal weight of the configuration using straight stiffeners. The optimal curvilinear stiffeners become almost straight like in the optimal configuration of

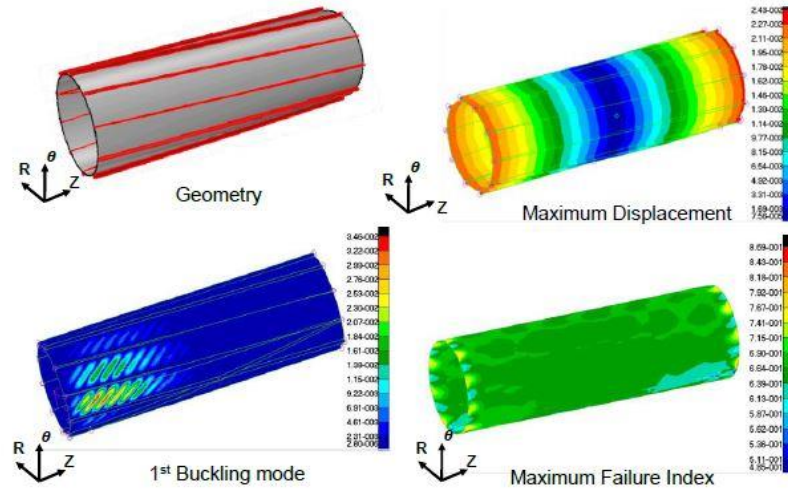


Fig. 10 Optimal configuration using curvilinear stiffeners under the torsional load case. (buckling factor = 1.004, maximum failure index = 0.869, stress factor (stiffeners) = 0.822, mass = 36.26 kg) the optimal cross-section dimensions are given in Table 7

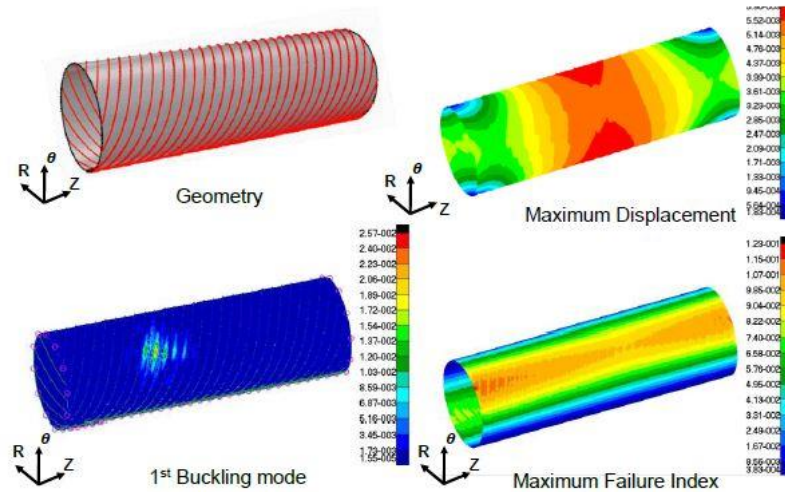


Fig. 11 Optimal configuration using curvilinear stiffeners under the bending load case. (buckling factor = 0.997, maximum failure index = 0.123, stress factor (stiffeners) = 0.916, mass = 32.20 kg) the optimal cross-section dimensions are given in Table 7

straight stiffeners. It should be noted that it is not possible to have a single hoop stiffener in the middle of the pipe using the parameterization of curvilinear stiffeners. These results show that in torsional load case, it is better to have straight stiffeners in comparison to the curvilinear stiffeners for reducing the overall weight of the structure. The optimal values of the design variables are tabulated in Table 7.

Fig. 11 shows the optimal configuration using curvilinear stiffeners under the bending load

Table 7 Optimal final values of design variables for the curvilinear stiffeners case

	Torsional Load Case	Bending Load Case
n_j	10	12
n_k	1	1
α_j (degrees)	87.53	22.50
α_k (degrees)	80.32	68.39
h_s (m)	4.349E-02	1.015E-02
t_s (m)	1.000E-03	1.000E-03
t_p (m)	7.218E-04	6.187E-04
Mass (kg)	38.26	32.20

Table 8 Comparison of different configuration under the bending load case

Design Case	Total Mass (kg)	% Saving
<i>Orthogonal</i>	36.10	-
<i>Curvilinear</i>	32.20	10.8

case. In this case, the buckling constraint is again active with the buckling factor of 0.997. The maximum failure index and the stress factor are 0.123 and 0.916. The optimal weight is 32.20 kg. This optimal weight is 10.8% less than the optimal weight using straight stiffeners under bending load case. This shows that the use of curvilinear stiffeners is beneficial for saving weight in the structure in comparison to the use of straight stiffeners.

6. Summary and future work

A BLP optimization framework for designing stiffened pipes or pressure vessels with curvilinear stiffeners is developed. An integrated optimization framework utilizing the scripting based language Python, NURBS based Rhinoceros 3D, MSC.PATRAN and MSC.NASTRAN has been developed. It is seen that placement of the stiffeners has significant influence on the buckling load of the stiffened cylindrical surface and this can be beneficial for saving weight by optimizing the stiffener's cross-section and composite skin laminate thickness. The optimization technique utilizes the combination of Particle Swarm Optimization (PSO) and Gradient Based Optimization (GBO). For each particle of PSO, optimal size design is obtained using GBO (MSC.NASTRAN SOL 200) subjected to buckling, stress and composite skin laminate failure constraint. The framework can be used to design curvilinear stiffeners under different applied loads at the ends of the pipes. There could be many load cases beyond the scope of this paper. There could be other gradient free optimization techniques, like Genetic Algorithm optimization, which could be alternative to the PSO in this framework. Two different approaches, orthogonally-placed stiffeners and curvilinearly-placed stiffeners on the surface of a cylindrical pipe, under torsional and bending load cases, have been considered to show the use of the presented framework. It is seen that in the torsional load case, it is beneficial to use straight stiffeners over curvilinear stiffeners for reducing the overall weight of the structure. However, in the bending load case, it is better to use curvilinear stiffeners over the straight stiffeners. It is seen that curvilinear stiffeners have a potential of saving

weight in the composite skin laminate by 10.8% and thus saving cost of material required for composite skin laminate, as compared to the case of using straight stiffeners.

Acknowledgments

The authors would like to thank Dr. Mohamed Jrad for assisting in running optimization in parallel on multiple machines to save computation time.

References

- Alcantar, V., Aceves, S.M., Ledesma, E., Ledesma, S. and Aguilera, E., (2017), "Optimization of Type 4 composite pressure vessels using genetic algorithms and simulated annealing", *Int. J. Hydrogen Energy*, **42**(24), 15770-15781. <https://doi.org/10.1016/j.ijhydene.2017.03.032>.
- Alcantar, V., Ledesma, S., Aceves, S.M., Ledesma, E. and Saldana, A., (2017). "Optimization of type III pressure vessels using genetic algorithm and simulated annealing". *International Journal of Hydrogen Energy*, **42**(31), 20125-20132. <https://doi.org/10.1016/j.ijhydene.2017.06.146>
- Chen, X., Wang, X., Qiu, Z., Wang, L., Li, X. and Shi, Q., (2018), "A novel reliability-based two-level optimization method for composite laminated structures", *Compos. Struct.*, **192**, 336-346. <https://doi.org/10.1016/j.compstruct.2018.03.016>
- Colombo, C. and Vergani, L. (2018), "Optimization of filament winding parameters for the design of a composite pipe", *Composites Part B: Eng.*, **148**, 207-216. <https://doi.org/10.1016/j.compositesb.2018.04.056>.
- Dorey, A., Murray, D., Cheng, J., Grondin, G. and Zhou, Z. (1999), "Testing and experimental results for NPS30 line pipe under combined Loads", *In Proceedings of the 18th International Conference on OMAE*.
- Kapania, R.K., Li, J. and Kapoor, H. (2005), "Optimal design of unitized panels with curvilinear stiffeners", *In AIAA 5th Aviation, Technology, Integration, and Operations Conference (ATIO)/16th Lighter-than-Air and Balloon Systems Conference*, AIAA 2005-7482. <https://doi.org/10.2514/6.2005-7482>.
- Kidane, S., Li, G., Helms, J., Pang, S.S. and Woldesenbet, E. (2003), "Buckling load analysis of grid stiffened composite cylinders", *Compos. Part B: Eng.*, **34**(1), 1-9. [https://doi.org/10.1016/S1359-8368\(02\)00074-4](https://doi.org/10.1016/S1359-8368(02)00074-4).
- Krikanov, A.A. (2000), "Composite pressure vessels with higher stiffness", *Compos. Struct.*, **48**(1-3), 119-127. [https://doi.org/10.1016/S0263-8223\(99\)00083-5](https://doi.org/10.1016/S0263-8223(99)00083-5).
- Limam, A., Lee, L.H., Corona, E. and Kyriakides, S. (2010), "Inelastic wrinkling and collapse of tubes under combined bending and internal pressure", *Int. J. Mech. Sci.*, **52**(5), 637-647. <https://doi.org/10.1016/j.ijmecsci.2009.06.008>.
- Liu, G., Wei, G. and Gao, H. (2019), "A novel structure of woven composite pressure pipes and its multi-scale analysis". *J. Textile Institute*, 1-10. <https://doi.org/10.1080/00405000.2019.1610204>.
- Paquette, J. and Kyriakides, S. (2006), "Plastic buckling of tubes under axial compression and internal pressure", *Int. J. Mech. Sci.*, **48**(8), 855-867. <https://doi.org/10.1016/j.ijmecsci.2006.03.003>.
- Parnas, L. and Katirci, N. (2002), "Design of fiber-reinforced composite pressure vessels under various loading conditions", *Compos. Struct.*, **58**(1), 83-95. [https://doi.org/10.1016/S0263-8223\(02\)00037-5](https://doi.org/10.1016/S0263-8223(02)00037-5).
- Singh, K., Zhao, W. and Kapania, R.K. (2017), "Optimal design of curvilinearly stiffened shells", *In the 58th AIAA/ASCE/AHS/ASC Structures, Structural Dynamics, and Materials Conference*, AIAA 2017-1830. <https://doi.org/10.2514/6.2017-1830>.
- Singh, K., Zhao, W., Jrad, M. and Kapania, R.K. (2019), "Hybrid optimization of curvilinearly stiffened shells using parallel processing", *J. Aircraft*, **56**(3), 1068-1079. <https://doi.org/10.2514/1.C035069>.
- Zhao, W. and Kapania, R.K. (2016), "Buckling analysis of unitized curvilinearly stiffened composite panels", *Compos. Struct.*, **135**, 365-382. <https://doi.org/10.1016/j.compstruct.2015.09.041>.

Zhao, W. and Kapania, R.K. (2019), "Bilevel programming weight minimization of composite flying-wing aircraft with curvilinear spars and ribs", *ALAA J.*, **57**(6), 2594-2608. <https://doi.org/10.2514/1.J057892>.

CC